Stability, Bonding, and Geometric Structure of Ti_8C_{12}, Ti_8N_{12}, V_8C_{12}, and Zr_8C_{12}

H. Chen, M. Feyereisen, X. P. Long, and G. Fitzgerald
Cray Research Inc., 655E Lone Oak Drive, Eagan, Minnesota 55121
(Received 17 March 1993)

We investigate the stability, bonding, and geometric structure of recently discovered metallocarbohedrenes by the use of density-functional calculations. It is found that the previously proposed T_h dodecahedron structure is dynamically unstable. Instead, a new, stable, and more strongly bound structure with D_{2d} symmetry is found. We find strong interactions between C-C and strong Ti-C covalent bonding. The stability of the D_{2d} structure has been verified by calculating vibrational frequencies. The infrared spectrum of the Zr_8C_{12} cluster is predicted.

PACS numbers: 61.46.+w, 31.20.Sy, 33.10.Gx, 36.40.+d

Since the discovery of C_{60}, substantial theoretical and experimental effort has been devoted to the study of fullerenes, fullerites, and other cagelike systems. Molecular clusters Ti_8C_{12}, Zr_8C_{12}, V_8N_{12}, and Hf_8C_{12} have been recently observed by Guo *et al.*, using laser vaporization techniques, to have exceptional stability and abundance [1]. These systems may be capable of exhibiting a rich variety of electronic and magnetic properties due to the presence of transition metal elements. Inspired by the analogy with C_{60} and in order to account for the observed stable ND_3 uptake by Ti_8C_{12}, Guo *et al.* have envisioned a cagelike dodecahedron structure with the T_h point group symmetry and proposed the name metallocarbohedrenes for these clusters. Subsequently, total-energy density-functional calculations carried out by Reddy, Khanna, and Jena [2] and Methfessel, van Schilfgaarde, and Scheffler [3] for the cluster Ti_8C_{12} conclude that the structure of Ti_8C_{12} is only slightly distorted from the perfect dodecahedron due to the difference between C-C and Ti-C interatomic distances, and the T_h symmetry remains stable and strongly bound. In this paper, we demonstrate that the previously proposed cagelike dodecahedron structure is energetically unstable against the Jahn-Teller distortion. Instead, a new, stable, and more strongly bound structure with the D_{2d} symmetry is obtained. Characters of interatomic bonding in this new structure are substantially different from those proposed for the dodecahedron by Guo *et al.*, which are based on the assumption that Ti and C are equal participants of twelve pentagon rings to form the dodecahedron [1]. Here, strongly covalent diatomic C-C bonding is observed. The newly found structure can be viewed as six pairs of C_2 dimers adsorbed on six surfaces of Ti_8 or Zr_8 clusters in the D_{2d} symmetry. Strong Ti-C bonding is due to the back donation of electrons from Ti to C_2 π_g orbitals. Through vibrational analysis, the infrared spectrum of the D_{2d} Zr_8C_{12} cluster is predicted. This will provide a crucial test of our theory when the corresponding experimental information becomes available.

The present study is based on spin-polarized density-functional total-energy calculations made with the use of the program package DGauss [4,5]. The computational method has been described previously [5,6]. In the present work, we have studied the following systems: Ti_8C_{12}, Ti_8N_{12}, V_8C_{12}, Zr_8C_{12}, and Zr_8. For Zr_8C_{12} and Zr_8 clusters, *ab initio* norm-conserving pseudopotentials [7] are used for the Zr atom. Other atoms are treated with the all-electron approach. The first order total-energy gradients are calculated analytically while the second order gradients are evaluated numerically. Geometry optimization is performed using analytic gradients and a quasi-Newton search algorithm as described in Ref. [8]. Several starting geometries were used by randomly displacing atomic positions in the T_h dodecahed-

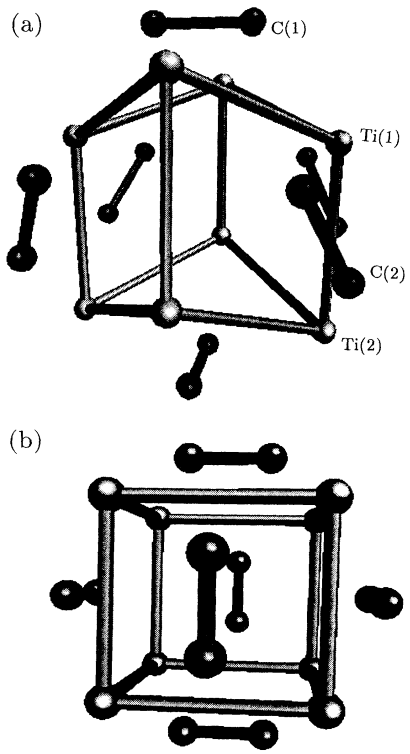

FIG. 1. (a) Geometric structure of the D_{2d} Ti_8C_{12} cluster. Ti atoms are at the corners of the gray cage. Carbon atoms are connected in dark pairs. (b) The structure of the T_h Ti_8C_{12} cluster.

0031-9007/93/71(11)/1732(4)$06.00

ron structure.

Our optimized geometry of Ti_8C_{12} is shown in Fig. 1(a). Ti_8N_{12}, V_8C_{12}, and Zr_8C_{12} all have the same structure, which has the D_{2d} point group symmetry. As a comparison, Fig. 1(b) shows the previously proposed T_h structure. Unlike in the T_h dodecahedron structure, where all Ti atoms are equivalent to each other, there are two types of Ti atoms in the D_{2d} structure, as marked in Fig. 1(a). There are four Ti(1) atoms each with five carbon nearest neighbors and four Ti(2) atoms each with four carbon nearest neighbors. In the T_h cluster, every Ti atom has only three carbon nearest neighbors. Eight Ti atoms form a cage of a distorted cube. In the T_h structure, eight Ti atoms form a perfect cube. Carbon atoms are also divided into two groups here. Two pairs of C(1) atoms are at the top and the bottom of Fig. 1(a). Four pairs of C(2) atoms are adsorbed onto the center of four parallelograms formed by the Ti_8 cage, with the C-C bond bridging along the longest diagonal. In the T_h dodecahedron structure, six pairs of C_2 are oriented toward the middle of the Ti-Ti bonds, while in the D_{2d} structure of Fig. 1(a), all C_2 dimers are oriented directly toward Ti atoms. An important element which led Guo *et al.* [1] to postulate the T_h dodecahedron structure for Ti_8C_{12} is the observation that this cluster can hold eight ND_3 molecules, implying that Ti atoms are at exposed positions. As can be seen from Fig. 1, all eight Ti atoms in the D_{2d} structure are exposed as well since this is a relatively small cluster. The D_{2d} structure can also adsorb eight ND_3 molecules. For the D_{2d} Zr_8C_{12} cluster, we have studied the binding of a NH_3 molecule onto either Zr(1) or Zr(2) sites. The NH_3 molecule is found to be more bound to the Zr(1) site with a binding energy of 1.43 eV. The binding energy is 1.30 for the Zr(2) site. The bond distance between Zr(1) and N is 2.35 Å, and 2.39 Å between Zr(2) and N. Since there is only a single NH_3 binding energy in the T_h structure, measurements of the binding energies will provide another crucial test of our prediction.

Our calculated structural data are presented in Table I. In addition to data for the D_{2d} structures, we have listed bond lengths of Ti_8C_{12} and Zr_8C_{12} optimized in the T_h symmetry. Bond distances of C-C and Ti-C calculated here for the T_h Ti_8C_{12} cluster are in excellent agreement with early reports [2,3]. Only the nearest neighbor distances are given in Table I. It is seen that bond distances are shorter in the D_{2d} symmetry than in the T_h symmetry. Ti-Ti distances are reduced by 10%. It was noticed previously that there is essentially no interaction between Ti atoms in the T_h Ti_8C_{12} structure [2]. Reduction of Ti-Ti distances certainly will increase the direct interaction between them. Distances between Zr atoms in the D_{2d} structure of Zr_8C_{12} are shortened by 8% from the T_h structure. We have optimized the geometry of a free Zr_8 cluster and found that it also has the D_{2d} symmetry. Nearest neighbor distances in the Zr_8 cluster are further reduced by 10%. Direct bonding between Zr atoms holds the Zr_8 cluster together, whereas in the Zr_8C_{12} cluster, Zr-C interactions contribute significantly to the cluster binding. C-C distances are also shorter in the D_{2d} structures. In fact, C-C distances of the D_{2d} structures are very close to the bond length (1.32 Å) of a free C_2 dimer. Strong C-C interaction has been previously observed in the T_h Ti_8C_{12} cluster in Ref. [3].

TABLE I. Bond distances (Å), binding energy per atom (eV), Mulliken charges, and Mayer bond orders of clusters. *M* stands for the transition metal; *A* stands for carbon or nitrogen. Numbers inside parentheses are results for the T_h structure.

	Ti_8C_{12}	Ti_8N_{12}	V_8C_{12}	Zr_8C_{12}	Zr_8
			Bond distances		
M(1)-*M*(2)	2.77(3.04)	2.60	2.62	3.00(3.25)	2.74
M(1)-*M*(2)	2.81(3.04)	2.61	2.57	3.03(3.25)	2.77
A(1)-*A*(1)	1.36(1.41)	1.42	1.39	1.37(1.43)	
A(2)-*A*(2)	1.37(1.41)	1.37	1.38	1.38(1.43)	
A(1)-*M*(1)	2.04(1.97)	2.06	1.89	2.18(2.09)	
A(1)-*M*(2)	2.09(1.97)	2.00	2.04	2.21(2.09)	
A(2)-*M*(1)	2.08(1.97)	2.10	2.04	2.21(2.09)	
A(2)-*M*(2)	1.95(1.97)	1.97	1.90	2.09(2.09)	
			Binding energies		
LSD	7.47(6.79)	6.54	7.00	7.37(6.60)	4.20
LSD+BP	6.54(5.95)	5.51	5.92	6.62(6.03)	3.69
			Charges		
M(1)	0.39(0.48)	0.79	0.16	0.42(0.50)	
M(2)	0.33(0.48)	0.62	0.18	0.43(0.50)	
A(1)	−0.22(−0.32)	−0.49	−0.11	−0.30(−0.33)	
A(2)	−0.25(−0.32)	−0.46	−0.12	−0.27(−0.33)	
			Bond orders		
M(1)-*M*(2)	0.45(0.33)	0.46	0.58	0.45(0.34)	
A(1)-*A*(1)	1.03(1.17)	0.80	0.73	1.07(1.12)	
A(2)-*A*(2)	1.09(1.17)	0.98	1.03	0.91(1.12)	
A(1)-*M*(1)	0.90(1.06)	0.55	1.19	0.84(1.06)	
A(1)-*M*(2)	0.63(1.06)	0.67	0.65	0.57(1.06)	
A(2)-*M*(1)	0.62(1.06)	0.38	0.54	0.57(1.06)	
A(2)-*M*(2)	1.12(1.06)	0.98	1.20	1.12(1.06)	

Table I also lists the cluster binding energies. LSD stands for binding energies obtained within the standard local spin density approximations to the exchange-correlation energy [9]. LSD+BP energies include nonlocal corrections of Becke [10] and Perdew [11] to the exchange-correlation energy. As expected, nonlocal binding energies are smaller than LSD results. This reduction of binding energies, however, is sufficiently uniform so that the overall trend of binding strength is not altered. Ti_8C_{12} and Zr_8C_{12} are the tightest bound clusters with binding energies per atom at about 7.4 eV. D_{2d} structures are more bound than T_h structures by nearly 0.8 eV/atom. The binding energy of 7.4 eV/atom is comparable to that of strongly bound bcc Nb (7.57 eV/atom) or diamond (7.37 eV/atom). The binding energies of gas phase N_2 and C_2 molecules are 4.9 and 3.2 eV/atom, respectively, which are smaller than the average binding en-

ergies of metallocarbohedrenes, indicating the strength of the interaction between transition metal and carbon or nitrogen. For the T_h Ti_8C_{12}, our calculated LSD binding energy of 6.8 eV/atom is in good agreement with earlier values of 6.6 eV/atom reported by Ref. [3] and 6.1 or 6.6 eV/atom by Ref. [2]. Replacing carbon by nitrogen appears to reduce the binding energy. However, Ti_8N_{12} remains strongly bound. Among the systems listed in Table I, Zr_8 has the smallest binding energy. Binding energies of other systems are greatly increased by metal-carbon and metal-nitrogen interactions.

We have calculated the total energies of the Ti_8C_{12} clusters—in both the D_{2d} and T_h symmetries—in several molecular spin states, each at their respectively optimized geometries. It is found that for either the D_{2d} or the T_h symmetry, the singlet spin state has the lowest total energy.

Following binding energies in Table I are atomic charges from the Mulliken analysis and the Mayer bond orders. About 0.4 electron from each transition metal atom in V_8C_{12} and Zr_8C_{12} clusters are transferred to carbon atoms. For the Ti_8N_{12} cluster, each Ti atom donates about 0.7 electron. This relatively larger charge transfer is consistent with the larger electronegativity of N. The charge transfer is also relatively larger in the T_h structure. From Table I, there appears to be a correlation between the cluster binding energy and the amount of charge transfer between transition metal and N or C. More ionic systems are less bound. The back donation of electrons from metals to carbon or nitrogen plays an important role in the binding of C_2 or N_2 dimers onto the transition metal surfaces. Such phenomena are rather commonly observed in chemisorption of C_2, N_2, and O_2 on transition metal surfaces [12]. As will be demonstrated below, transferred electrons tend to occupy the antibonding π_g orbitals of C_2 and N_2 dimers; C-C distances are thus longer in the T_h structure. From the bond orders listed in Table I, it is seen that each C atom is not equivalently bonded to its three Ti neighbors. The Ti-C bond along the C-C direction is stronger than the other two Ti-C bonds. A strong dimer C-C bond is also evident. The strength of the C-C bond is nearly the same as the strongest Ti-C bonds. The vibrational analysis to be discussed below also indicates strong C-C bonding. The Zr_8C_{12} cluster shows modes which can be easily identified with the C-C stretching vibrations. As the Ti-Ti distance is smaller in the D_{2d} structure, the direct Ti-Ti bond order is therefore larger. Unlike in the Ti_8C_{12} or Zr_8C_{12} clusters, where the C(1)-C(1) and C(2)-C(2) bond orders are very similar, the C(1)-C(1) bond order in the V_8C_{12} cluster is considerably smaller than that of the C(2)-C(2) bond.

If additional electrons are introduced to a free C_2 dimer, they will occupy the bonding orbitals formed from carbon p atomic states. But on a Ti surface, strong carbon p and titanium d hybridization lowers the antibonding π_g orbitals of C_2. Transferred electrons will occupy

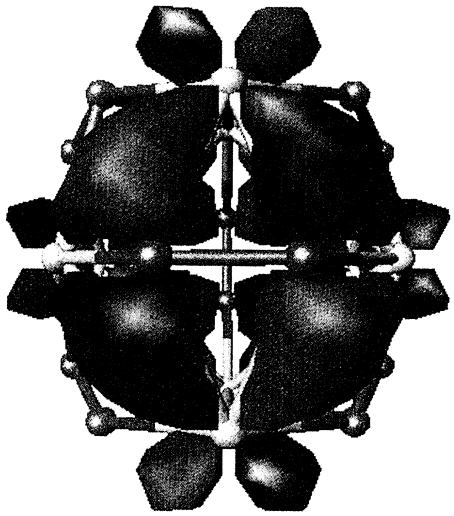

FIG. 2. Constant-value surfaces of a cluster wave function whose energy is 1.5 eV below E_F. Red surfaces for positive $\psi(\mathbf{r})$ at 0.1 $Å^{-3/2}$; purple surfaces for negative wave function at -0.1 $Å^{-3/2}$. The perceptive angle is vertical to that of Fig. 1 (a top view of Fig. 1).

these states to strengthen the C-Ti bonding. To illustrate this bonding effect, Fig. 2 shows the molecular orbital for a state that is at 1.5 eV below the Fermi level. The perception angle is different in Fig. 2. Here, a vertical view of Fig. 1 is presented. Two green dots in the middle of Fig. 2 are the C(1) atoms; yellow dots, Ti atoms. Constant-value surfaces of the wave function at $+0.1$ $Å^{-3/2}$ are shown in red. Purple surfaces represent the wave function at -0.1 $Å^{-3/2}$. The shape of the wave function around two C(1) atoms is clearly of the π_g character, which helps the formation of strong bonding orbitals between C p and four neighboring Ti d states. Comparing the interatomic bonding in C_{60} or graphite with that in Ti_8C_{12}, two basic differences are prominent. (1)

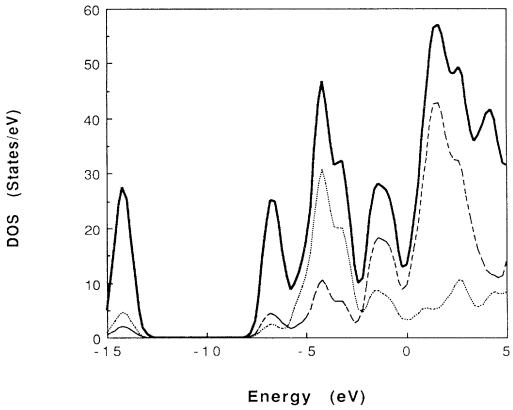

FIG. 3. Density of states of the D_{2d} Ti_8C_{12}. Thick line is the total DOS. Dotted line is for C p components. Dashed line is for Ti d components. The Fermi level is shifted to $E=0$.

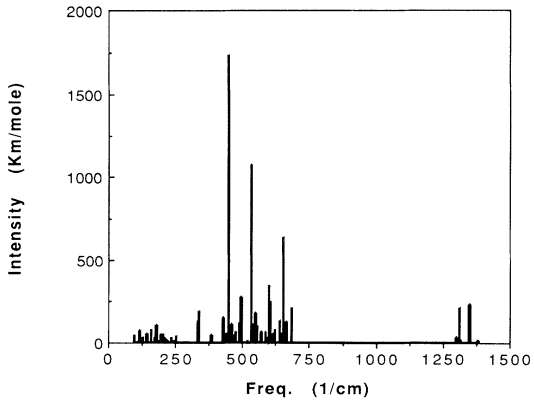

FIG. 4. Infrared spectrum of the D_{2d} Zr_8C_{12} cluster.

In C_{60} or graphite, antibonding orbitals π_g are never occupied since there are no additional charges. (2) Bonds between neighboring atoms in C_{60} or graphite are σ bonds of sp^2 hybridized orbitals and the π bonds of p_z orbitals, while in Ti_8C_{12} or its variations discussed in this paper, C_2 and N_2 bonds have antibonding components in addition to the bonding orbitals that are present in free C_2 and N_2 dimers and C-Ti bonding is primarily of σ bonding between Ti d and C_2 π_g orbitals as shown in Fig. 2.

That there is strong covalent bonding between Ti d and C p states can also be inferred from the plot of the density of states shown in Fig. 3. Two low energy peaks at 14.2 and 6.8 eV below the Fermi energy are due to C $2s$ states. Carbon p states peak at 4.2 eV below E_F. States around this peak are mainly carbon π_u bonding orbitals which, together with σ_g bonds of C $2s$, are responsible for the interatomic C-C binding. It is seen from Fig. 3 that at higher energies carbon p states are delocalized and an appreciable amount of C p states are spread in a wide range of energies around E_F. The majority of Ti d states are above the Fermi level. The peak at 1.4 eV below E_F has a substantial amount of Ti d components and shows strong C-p-Ti-d resonance. The strong C-Ti bonding is primarily due to these states. The spatial distribution of such a hybridized state in the center of this peak is shown in Fig. 2.

We now wish to consider aspects of stability and molecular vibrations which were neglected in previous studies [1–3]. Second order gradients are necessary, and we evaluated them numerically based on analytical first order gradients. Only the Zr_8C_{12} cluster is considered here with the help of pseudopotentials on Zr atoms to reduce the computational time. It is expected that our main conclusion regarding the stability will be valid for V_8C_{12} and Ti_8C_{12} clusters as well. We have found that the Zr_8C_{12} cluster in the T_h symmetry is unstable. Twelve imaginary frequencies were obtained from the dynamic matrix. The situation is a typical example of the Jahn-Teller effect. In the T_h molecular symmetry, the symmetry of the state at the Fermi level is found to be T_g, which is triply degenerate; yet there are only two electrons, four including both spins, to occupy these states. It is energetically favorable to distort the T_h molecular symmetry into the D_{2d} symmetry, thus splitting the T_g state into B_2 and E states. In addition, atoms in the D_{2d} structure have higher coordination numbers which enhance the interatomic interactions as demonstrated above. For the Zr_8C_{12} cluster in the D_{2d} symmetry, all its vibrational modes are stable with real frequencies. The lowest vibrational frequency is 96.7 cm^{-1}. We present the calculated infrared spectrum in Fig. 4. Infrared intensities are calculated using the derivatives of dipole moments. Three strongest infrared modes are at 449.0, 534.0, and 653.1 cm^{-1}. In the vibrational spectrum shown in Fig. 4, there are six high-frequency modes ranging from 1302 to 1382 cm^{-1}, which are well separated from the other modes by about 610 cm^{-1}. Analysis of the vibrational eigenvectors shows that they correspond to six pairs of C-C stretching modes, indicating the presence of C_2 dimer character in the D_{2d} Zr_8C_{12} cluster. As a comparison, the stretching frequency of a free C_2^{-1} dimer is 1777 cm^{-1}. The C-C bond strength has been weakened.

To summarize, we have carried out density-functional total-energy calculations for several metallocarbohedrenes: Ti_8C_{12}, Ti_8N_{12}, V_8C_{12}, and Zr_8C_{12}. Contrary to previous suggestions, we find the T_h dodecahedra structure to be unstable against the Jahn-Teller distortion. A stable and more bound structure with the D_{2d} symmetry is found. Strong interatomic bonding is primarily due to strong C-C dimer interactions and covalent bonding between Ti d and C_2 π_g orbitals.

[1] B. C. Guo *et al.*, Science **255**, 1411 (1992); **256**, 515 (1992); J. Chem. Phys. **97**, 5243 (1992).
[2] B. V. Reddy, S. N. Khanna, and P. Jena, Science **258**, 1640 (1992).
[3] M. Methfessel, M. van Schilfgaarde, and M. Scheffler, Phys. Rev. Lett. **70**, 29 (1993).
[4] DGauss is a density-functional electronic structure software product available from Cray UniChem™ Project. UniChem is a trademark of Cray Research, Inc.
[5] J. Andzelm and E. Wimmer, J. Chem. Phys. **96**, 1280 (1992).
[6] H. Chen, M. Krasowski, and G. Fitzgerald, J. Chem. Phys. **98**, 8710 (1993).
[7] N. Troullier and J. L. Martins, Phys. Rev. B **43**, 1993 (1991).
[8] J. D. Head and M. C. Zerner, Adv. Quantum Chem. **20**, 239 (1989).
[9] S. H. Vosko, L. Wilk, and M. Nusair, Can. J. Phys. **58**, 1200 (1980).
[10] A. Becke, Phys. Rev. A **38**, 3098 (1988).
[11] J. Perdew, Phys. Rev. B **33**, 8822 (1986).
[12] T. H. Upton, P. Stevens, and R. J. Madix, J. Chem. Phys. **83**, 3988 (1988).

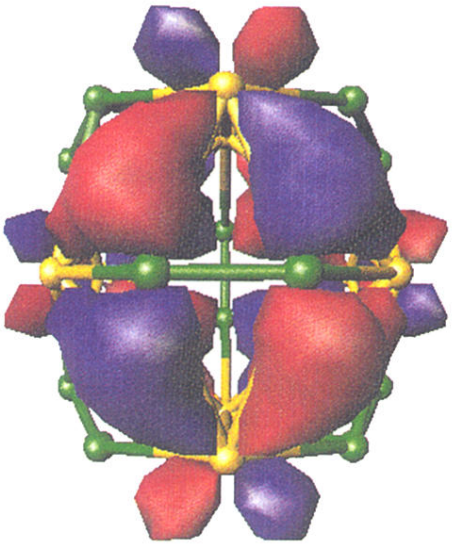

FIG. 2. Constant-value surfaces of a cluster wave function whose energy is 1.5 eV below E_F. Red surfaces for positive $\psi(\mathbf{r})$ at 0.1 $\text{Å}^{-3/2}$; purple surfaces for negative wave function at -0.1 $\text{Å}^{-3/2}$. The perceptive angle is vertical to that of Fig. 1 (a top view of Fig. 1).